

# Novel Infrared Phototransistors for Atmospheric CO<sub>2</sub> profiling at 2 $\mu$ m Wavelength

Tamer F. Refaat<sup>1</sup>, M. Nurul Abedin<sup>2</sup>, Oleg V. Sulima<sup>3</sup>, Upendra N. Singh<sup>2</sup> and Syed Ismail<sup>2</sup>

<sup>1</sup> Science and Technology Corporation, NASA Langley Research Center  
MS 468, Bldg 1202, Rm 243, Hampton, Virginia 23681

<sup>2</sup> NASA Langley Research Center, Hampton, Virginia 23681

<sup>3</sup> University of Delaware, Newark, Delaware 19716

## Abstract

Two-micron detectors are critical for atmospheric carbon dioxide profiling using the lidar technique. The characterization results of a novel infrared AlGaAsSb/InGaAsSb phototransistor are reported. Emitter dark current variation with the collector-emitter voltage at different temperatures is acquired to examine the gain mechanism. Spectral response measurements resulted in responsivity as high as 2650 A/W at 2.05  $\mu$ m wavelength. Bias voltage and temperature effects on the device responsivity are presented. The detectivity of this device is compared to InGaAs and HgCdTe devices.

## Introduction

Knowledge of the spatial and temporal distribution of atmospheric carbon dioxide (CO<sub>2</sub>) is important for understanding its impact on global warming and climate changes (1). Recent progress in 2  $\mu$ m tunable laser, where strong CO<sub>2</sub> lines are available, drives the need for high quality detectors operating at the same wavelength. Such technology would allow the application of high resolution remote sensing techniques such as the Differential Absorption Lidar (DIAL) for profiling and monitoring CO<sub>2</sub> in the atmosphere (2).

An ideal detector for this application would have high quantum efficiency with high gain, low noise and narrow spectral response peaking around the wavelength of interest. This increases the DIAL instrument signal-to-noise ratio while minimizing the background signal, thereby increasing the sensitivity and dynamic range besides reducing its mass and cost for space missions. Commercially available extended wavelength InGaAs and HgCdTe detectors provide 2- $\mu$ m sensitivity, but due to the absence of internal gain mechanism, they lack sufficient responsivity. Avalanche photodiodes (APD) based on InGaAsSb quaternary alloy indicated promising performance for 2- $\mu$ m detectors (3, 4), but they suffer relatively low signal-to-noise ratio and they are not commercially available. On the other hand similar arguments apply for the 1.3- and 1.5- $\mu$ m applications, where phototransistors are competitive to photodiodes. High gain phototransistors lack the need for high base voltage and do not suffer the excess noise effects that APDs have (5).

In this paper, the characteristics of novel heterojunction AlGaAsSb/InGaAsSb infrared phototransistors are reported (6, 7). The characteristics include dark current measurement and responsivity variation with bias voltage and temperature. The detectivity results are presented and are compared to mature InGaAs and HgCdTe detector technologies.

## Two Micron Phototransistor Structure

The device structure is shown in Fig. 1. The structure includes an n-type AlGaAsSb emitter, p-type composite base consisting of AlGaAsSb and InGaAsSb layers, and an n-type InGaAsSb collector. All layers were lattice-matched to a GaSb substrate and were grown by liquid-phase epitaxy using a horizontal slideboat technique. The bandgap energies of the AlGaAsSb and InGaAsSb layers are 1–1.1 eV and 0.55 eV, respectively, as estimated from the chemical composition and spectral response measurements (7). Mesa phototransistors with a 400  $\mu$ m diameter total area and a 200  $\mu$ m diameter active area were defined using photolithography and wet chemical etching. A backside planar and a front side annular ohmic contact, including a bonding pad, were deposited by electron beam evaporation of Au/Sn and Ti/Ni/Au, respectively. A polyimide coating (HD Microsystems PI-2723 photodefinable polyimide resin) was spun on the front of the device. The polyimide serves several functions including planarization of the top surface, mesa isolation and edge passivation. After dicing, 1 mm<sup>2</sup> pieces with a single device in the middle of each square were mounted on to TO-18 headers using silver conducting epoxy and wire-bonded. No antireflection coatings were applied.

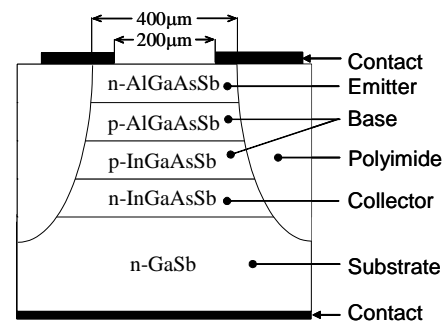


Fig. 1. Schematic of the infrared AlGaAsSb/InGaAsSb phototransistor structure.

## Experimental Setup

Several prototype InGaAsSb/AlGaAsSb phototransistors were fabricated and characterized in order to compare their performance with existing 2- $\mu\text{m}$  detector technologies beside the requirement of the CO<sub>2</sub> DIAL measurements. The characterization experiments included emitter dark current, responsivity and noise measurements. Fig. 2 shows the experimental setup used to obtain these characteristics. The setup is divided mainly into optical, electrical and detector control sections. The optical section is used to apply a uniform, monochromatic radiation onto the detector, with known intensity. The electrical section mainly measures the detector output, corresponding to a certain operating conditions, while maintaining these conditions using the detector control section.

### A. Optical Section

In the optical section, the radiation source consists of a current controlled quartz halogen lamp, the output of which is modulated using an optical chopper. The chopping frequency is set to a prime number of 167 Hz to reduce the effect of pickup noise. A monochromator is used to separate the radiation into its spectral components with a 20 nm resolution as set by the input/output slits and the grating. Higher order dispersion of the shorter wavelength is blocked using appropriate high-pass filters, while a diffuser is mounted at about 10 cm from the detector to insure radiation uniformity. An optical microscope was used to set the location of the optical axis and to fix the distance between the radiation source and the sensitive area of the detector. The radiation uniformity is estimated to be less than 1% along a 15 mm<sup>2</sup> area at the detector location.

### B. Electrical Section

The detector output current is converted into voltage signal using the pre-amplifier (Stanford Research Systems; SR570), the output of which is applied to a lock-in amplifier (Optronic Laboratories, Inc.; OL 750-C), oscilloscope (Agilent; infiniiium) or spectrum analyzer (Stanford Research Systems; SR785), for responsivity and noise measurements. For emitter dark current measurements, a modular dc source/monitor (Hewlett Packard; 4142B) is connected directly to the detector. The chopper controller synchronizes the applied optical signal, if any, with the data acquisition device through the personal computer.

### C. Detector Control Section

The detector is mounted inside a chamber that controls its temperature and provides mechanical support. For high temperature operation down to  $-23\text{ }^{\circ}\text{C}$ , an open chamber is used. In the open chamber the temperature is controlled using thermoelectric coolers and a thermistor, located as close as possible to the device. Water circulation through a chiller removes excess heat accumulation and nitrogen purging prevents water condensation and ice formation on the detector surface at temperatures below  $0\text{ }^{\circ}\text{C}$ . For lower temperature operation, a cryogenic chamber is used with liquid nitrogen as the cooling media, with vacuum isolation and a controlled resistive heater to set the temperature. To bias the detector, the pre-amplifier is used for voltages in the 0 to 4 V range while the external dc power supply is used for higher voltages. Mechanical mount allows detector alignment within 10  $\mu\text{m}$  resolution.

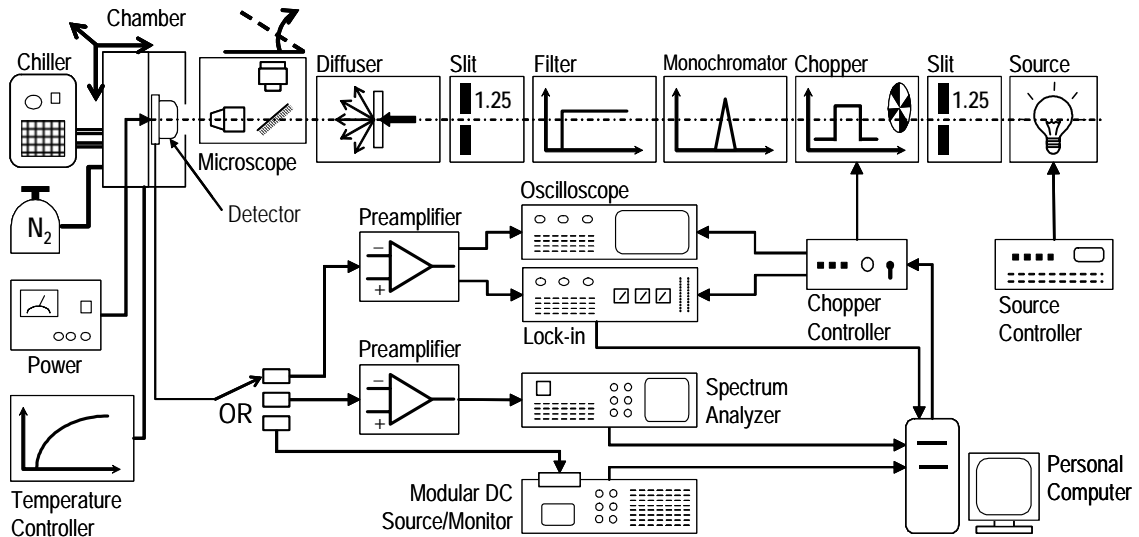


Fig. 2. Experimental Setup for phototransistor dark current, spectral response and noise measurements, in the 77 to  $-193^{\circ}\text{C}$  temperature range.

## Characterization Results

Fig. 3 shows the emitter dark current variation with the collector-emitter voltage at different temperatures. Emitter dark current was obtained by I-V measurements in dark conditions by applying the bias voltage to the emitter while the collector contact connected to the ground. Two current regions were observed in these characteristics. The first region, where 0- to 1.5-V was applied, is characterized by a relatively low current with strong temperature dependence. At higher voltage, above 1.5 V, a sharp increase in the dark current with lower temperature dependence and high current-voltage linearity is observed. Emitter dark current measurements reveal the absence of any avalanche gain.

The device spectral response peaks around the 2- $\mu\text{m}$  wavelength, which is optimal for the CO<sub>2</sub> measurements (7). Therefore, responsivity variation with bias voltage and temperature are presented at 2.05  $\mu\text{m}$ . At this particular wavelength strong CO<sub>2</sub> absorption line exist with minimal influence from other species, such as water vapor. Figure 4 shows the responsivity variation with the collector-emitter voltage at different temperatures for two phototransistor samples (A1-b1 and A1-d2). As a general trend, sharp increase in the responsivity at lower bias voltage is observed, followed by a knee then saturation at higher voltage. Figure 5 shows the responsivity variation with the temperature at different collector-emitter voltages for the same samples. The results indicate complicated temperature dependence with a low responsivity peak around -120 °C and higher increase at higher temperatures. Responsivity as high as 2650 A/W, corresponding to an internal gain of 2737, was measured with phototransistor A1-b1 at 2.05  $\mu\text{m}$ , -20°C and 4.5 V.

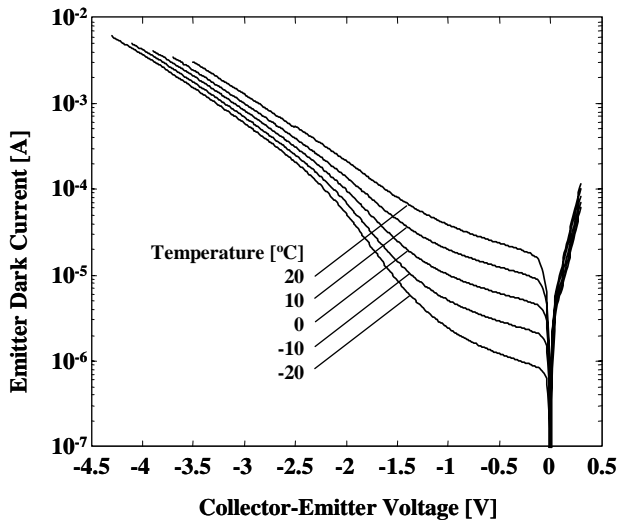


Fig. 3. Emitter dark current variation as a function of collector-emitter voltage at different temperatures.

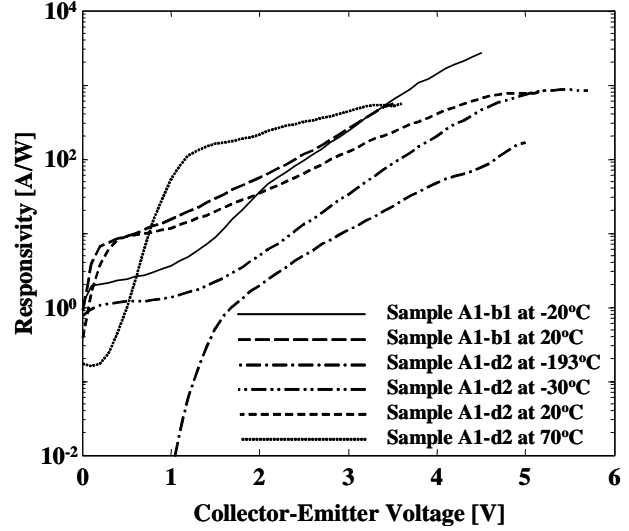


Fig. 4. Responsivity variation with bias voltage and temperature by using 2.05  $\mu\text{m}$  laser radiation

Fig. 6 shows the detectivity calculation of two phototransistors (samples A1-d2 and A1-a2) as compared to the state-of-the-art, 1 mm diameter InGaAs and HgCdTe photodiodes, listed in table I. Detectivity calculation was obtained using noise measurements in the dark conditions and spectral response data (detail discussion in ref. 7). The figure also compares the results with the ideal background limited detectivity, assuming black body source at -20 °C, with 180° detector field-of-view. All results obtained at -20 °C, and -193 °C was only considered for A1-a2 sample to emphasis cooling improvements. Cooling down the device reduces the dark current, which allows for higher voltage operation leading to increase the responsivity. Besides, cooling reduces the dark noise leading to increase the detectivity for shorter wavelength. For the shown curve, the peak detectivity of  $1.6 \times 10^{13} \text{ cm} \cdot \text{Hz}^{1/2} / \text{W}$  was shifted to 1.85- $\mu\text{m}$  at 5.0 V bias. An optimization would be required to identify a suitable operating temperature while avoiding the responsivity drop due to the cut-off wavelength shift at lower temperatures. The operating bias voltage for the commercial detectors was 1 V as specified by the manufactures. It should be noted that increasing the bias voltage for the commercial detectors significantly increases the noise, leading to detectivity deterioration.

Table I Two micron commercial detectors used for comparison with the new phototransistor. The detectors obtained with 1 mm diameter and operated at 1 V bias and -20 °C.

Material	Manufacturer	Part #	Structure	Cut-off
InGaAs	Hamamatsu	G5852	pin	2.3 $\mu\text{m}$
InGaAs	Hamamatsu	G5853	pin	2.6 $\mu\text{m}$
HgCdTe	Judson	J19:2.8-18C-R01M	pn	2.8 $\mu\text{m}$

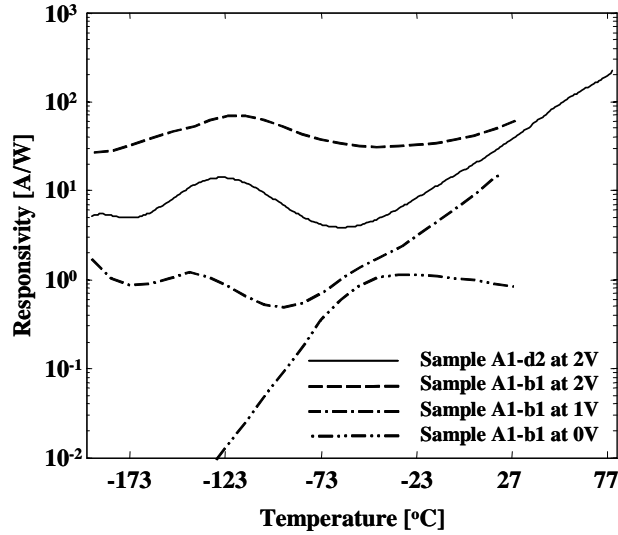


Fig. 5. Responsivity variation at  $2.05\ \mu\text{m}$  as a function of temperature at different bias voltages for Samples# A1-d2 and A1-b1

### Conclusion

AlGaAsSb/InGaAsSb based phototransistors were optimized for  $2\ \mu\text{m}$  remote sensing applications. The experimental setup for characterizing the new devices was presented. Emitter dark current measurements indicates relatively low current values, which further reduced by cooling. The results reveal the absence of avalanche gain. Responsivity variation with bias voltage and temperature indicated a complex dependence on the device operating conditions. Further studies are necessary to understand the origin of this behavior. In the range of typical terrestrial temperature and at bias voltages exceeding several tenths of volt, increase of responsivity both with temperature and voltage is observed. The new phototransistor showed superior detectivity compared to standard InGaAs and HgCdTe photodetectors. With relatively low dark current and high responsivity, signal-to-noise ratio improvements meet the requirement of the  $\text{CO}_2$  measurement using the DIAL technique. Optimization of the transistor operating bias voltage and temperature should be attempted for this application.

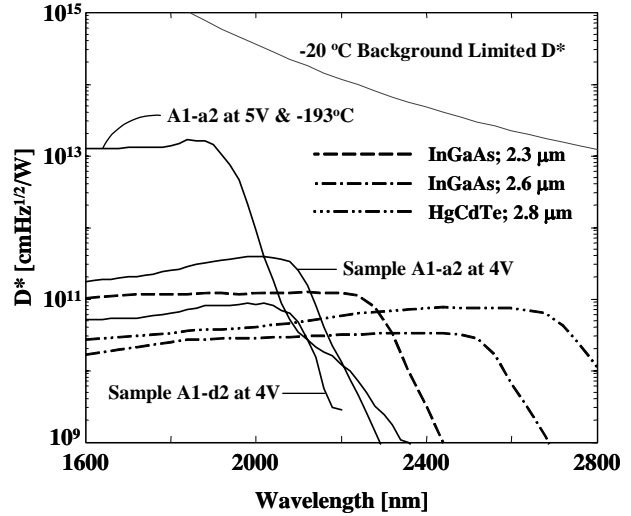


Fig. 6. Detectivity comparison of phototransistors at  $-20^\circ\text{C}$  with respect to commercially available photodiodes at the same temperature. Also shown is  $D^*$  of the phototransistor A1-a2 at  $-193^\circ\text{C}$ .

### Acknowledgement

This effort is part of the Laser Risk Reduction Program funded by NASA's Earth Science Technology Office and NASA's Enabling Concepts and Technologies Program. The authors would like to thank George Komar, Chris Moore, and Frank Peri for their constant support.

### References

- (1) J. Kaiser and K. Schmidt, *Science*, **281**, 504, 1998.
- (2) P. F. Ambrico, A. Amodeo, P. D. Girolamo and N. Spinelli, *Appl. Opt.*, **39**, 6847-6865, 2000.
- (3) A. Andreev, M. A. Afrailov, A. N. Baranov, M. A. Mirsagatov, M. P. Mikhailov, and Y. P. Yakovlev, *Sov. Tech. Phys. Lett.*, **14**, 435-437, 1988.
- (4) O.V. Sulima, M.G. Mauk, Z.A. Shellenbarger, J.A. Cox, P.E. Sims, S. Datta, and S.B. Rafol, *IEEE Proceedings – Optoelectronics*, **151**, 1-5, 2004.
- (5) J.C. Campbell, A.G. Dentai, C.A. Burrus, and J.F. Ferguson, *IEEE J. Quantum Electronics*, **17**, 264, 1981.
- (6) O.V. Sulima, T.F. Refaat, M.G. Mauk, J.A. Cox, J. Li, S.K. Lohokare, M.N. Abedin, U.N. Singh, and J. A. Rand, *Elect. Lett.*, **40**, 766-767, 2004.
- (7) T. F. Refaat, M. N. Abedin, O. V. Sulima, S. Ismail, and U. N. Singh, *Opt. Eng.*, **43**, 1647-1650, 2004.